PCCP

Condensation and Growth of Amorphous Aluminosilicate Nanoparticles by Aggregation Process

Condensation and Growth of Amorphous Aluminosilicate Nanoparticles by Aggregation Process

Romain Dupuis,[1, *] Seung Ho Hahn,[2] Adri C.T. Van Duin,[2] Roland Pellenq,[3] and Arnaud Poulesquen[4]

[1] *Université de Montpellier - IEM and ICGM, Montpellier, France*

[2] *Department of Mechanical Engineering, Pennsylvania State University, University Park PA 16802, USA*

[3] *International Research Laboratory, EPIDAPO, CNRS-George Washington U., Washington DC*

[4] *CEA, DES, ISEC, DE2D, SEAD, LCBC, Univ Montpellier, Marcoule, France*

(Dated: February 28, 2022)

Abstract

The precipitation of zeolite nanoparticles involves the initial formation of metastable precursors such as amorphous entities that crystalize through non-classical pathways. Here, using reactive force field based simulations, we reveal how aluminosilicate oligomers grow concomitantly to the decondensation of silicate entities during the first step of the reaction. Aluminate clusters first form into the solution, thus violating the Lowenstein's rule in the first instant of the reaction, followed by the connection with silicate oligomers at the dead-end silanol group and then reorganize to finally diffuse within the silicate oligomers to form stable amorphous aluminosilicate nanoparticles respecting the Lowenstein rule. Our results clearly indicate that the aluminate does not serve as the neuralgic center for the growth of aluminosilicate in a nucleation-like process but rather acts as an aggregation process. The coexistence of aluminosilicate oligomers and small silicate entities induces a phase separation promoting the precipitation of zeolites with aging.

Zeolites and alkali activated materials (AAM) are both aluminosilicate materials resulting from the polycondensation of silicate and aluminate entities at the atomic scale. Silicates in alkali solution possess a certain degree of connectivity forming dimers, trimers, rings, or larger oligomers and the protonation rate depends on the nature of the alkali cation and the hydroxide content[1, 2]. On the other hand, aluminum in alkali solution occupies, as the silicon, tetrahedral coordination sites but remains under monomeric shape $[Al(OH)_4]^-$ [3]. Alkali cations compensate either the negative charge of the aluminum or form ion pairing with the deprotonated silicate[4]. Mixing alkali silicate with alkali aluminate solution results in the production of polydisperse aluminosilicate entities that grow and aggregate over time to form an amorphous hydrogel[5] or a clear solution, according to the initial concentration of the precursors, that crystallizes into zeolites usually after a hydrothermal treatment[6–8]. In the process of zeolite synthesis, aluminates are often directly available to react with the silicates in solution whereas in the case of AAM (also named geopolymer), the aluminum is slowly released into the solution due to the dissolution of a solid aluminosilicate source as metakaolin[9–11] or by-products such as slag or fly ashes[12]. An aluminosilicate gel is therefore formed in the bulk around the clay particles[13] and grows over time due to the dissolution reactions that last few days. At the molecular scale, the interaction between aluminate and silicate is still to be clarified since they are the precursors of aluminosilicates

---

* romain.dupuis@umontpellier.fr

gels that produce zeolites or AAM.

The early stages of the formation of aluminosilicates have been studied by atomistic simulations to understand the localization of aluminum in the chains, showing the importance of the Loweinstein rule (Si-O-Al linkages are favored energetically over Al-O-Al linkages in aluminosilicates) as well as the role of charges and pH on the formation of clusters[14–19]. There is still a lot of information to unveil, in particular on how those clusters grow in solution. Chemical reactions are complex to simulate via atomistic simulations but they have to be considered to investigate each mechanism of this process separately. Recently, several methods have been suggested to accelerate the dynamics and observe the formation of silica-based materials including glasses, gels, and solutions[20–23] Using one of those reactive models we have shown that adding sodium hydroxide to a silicate solution induces the decondensation of the silicate in complete agreement with time-resolved SAXS experiments[21, 24].

In this letter, we are investigating the aggregation process between some silicate entities and aluminate monomers in an alkali-rich solution. Our experimental and theoretical results are in good agreement and indicate a complex reactional path leading to the formation of a biphasic system.

Initially, the solution that is studied here is a mix of a silicate solution with an aluminate solution, both solutions containing sodium hydroxide. The mixed solution has final concentrations of $[\text{Si}] = 1.125$ mol.L^{-1}, $[\text{Na}] = 1.31$ mol.L^{-1}, $[\text{Al}] = 0.12$ mol.L^{-1}. After the mixing, decondensation of silicate chains due to the presence of sodium hydroxide [21] and condensation of aluminosilicate species happen simultaneously[25]. Simulations are used to distinguish different mechanisms of the aluminosilicate formation, at the atomic scale, that can not be observed directly experimentally because of the involved time-scale that are not compatible with experimental devices. The results are compared to structural measurements (at equilibrium from an experimental point of view: minute time scale) and several key aspects of the simulation are in very good agreement with the experiments. The mechanism, reaction paths, speciation, and connectivity are extracted from the dynamics and analyzed.

The solution has been simulated by accelerated molecular dynamics using the brief-parallel tempering (PT) method described in Dupuis et al.[21, 22] starting at the moment of the mixing (with no connectivity between aluminates and silicates) up to the formation of aluminosilicate clusters. This method has shown efficiency to increase the formation of solid species in solution. In particular because, contrarily to the usual PT, brief-PT is regularly

interrupted and the lowest temperature configuration is used to repopulate all the other temperatures. This bias is useful for liquids because it helps to avoid situations in which the configurations for two different temperatures are too different – which is likely due to the high number of configurations and that reduces the probability of exchanges in the PT technique. It is also very efficient compared to high-temperature MD [20]. The simulations have been performed using the LAMMPS package[26]. Each system has been simulated at constant temperature and volume using nosé-hoover thermostat as implemented in LAMMPS with a damp value of 100*dt. The parameters for the brief-PT are the following: the timestep was set to 0.25 fs, in order to properly describe the motion of water molecules with ReaxFF [27]; 16 temperatures have been used ranging from 300K to 1500K; the length of each parallel tempering was 1000 steps; every 50 steps an exchange of replica was attempted. The system size is 42x42x42 Å^3 and it contains about 2200 water molecules, 50 Si and 6 Al atoms with a density of 1.01 g.cm^{-3}.

The interaction between atoms in our MD simulation work has been treated using the ReaxFF reactive force field (the parameter set that has been used is attached as a S.I. file). ReaxFF is a bond-order dependent potential that can feature the formation and dissociation of bonds and thus, is perfectly suitable for studying the formation mechanism of aluminosilicates in the alkali-rich solution. The parameter set used herein is a combination of Na/Si/O/H ReaxFF parameterization[28] and Si/Al/O/H ReaxFF parameterization[29], which essentially shares the same Si/O/H interactions. The validity of this particular set of parameters has been reported in two distinct studies by Liu et al,. [30] which discusses the structural feature of aluminosilicate glass network consisting of Si-O-Si, Si-O-Al, and Al-O-Al and by Muraleedharan et al. [31] which elucidated the sodium transport dynamics of Na-montmorillonite and vibrational features of Si-O-Si, Si-O-Al bonds. The dynamics and chemistry discussed are similar to our system of interest in this study, and ensures that our ReaxFF parameter set is suitable for studying the growth kinetic of aluminosilicates in the solution environment under varying temperatures. Further details on the ReaxFF potential can be referred to the above-mentioned publications.

In the very beginning of the simulation, we observe that the aluminates, which were spread randomly within the simulation cell, quickly connect together and form small 3-members aluminate clusters. This is in agreement with ab initio calculations that have shown that 3-members aluminate clusters are stable in vacuum [32].
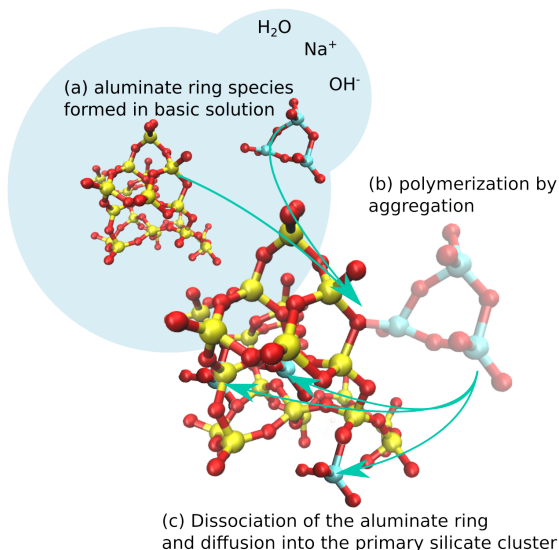
Figure 1. The formation of aluminosilicate species in a sodium-rich solution at high pH: (a) in solution, aluminates form small and stable clusters; (b) an aluminate cluster reacts with a primary silicate cluster in violation of the Loweinstein rule (the aluminosilicate contains Al-O-Al bridges); (c) the aluminate ring immediatly becomes unstable and dissociates at the surface of the primary silicates, each individual aluminate start diffusing into the structure. After 10ps, the Loweinstein rule is respected again and after 50ps, aluminates are in Q^4 sites.

The aluminate rings that are formed in solution remain stable at high pH as long as they remain independent and non-connected to silicates. We have found no events in which the aluminate ring opens and closes again, in contrast with what is observed for the silicate species[22]. Since the encounter probability between two $[Al(OH)_4]^-$ monomers and between $[Al(OH)_4]^-$ and $[Si(OH)_4]$ is similar, this indicates that the energy barrier to form Al-O-Al bonds is smaller than the one to form Al-O-Si bonds. To confirm this, we have calculated the energy along the reaction path to form a dimer from two monomers by adding an attractive force between an Si (or Al) atom and an O atom to force the reaction. The energy barrier is 30 kJ.mol^{-1} for Al-O-Al bonds and is 55 kJ.mol^{-1} for Al-O-Si bonds. This increase in the energy barrier is consistent with DFT calculations[33]. Note that in the literature, the energy of enthalpy of reaction show significant variability depending on the bond network and on the environment[14, 16].

The formation of aluminates in solution prior to the formation of aluminosilicates draws interrogations on how the Loweinstein rule will be respected in this aluminosilicate forma-
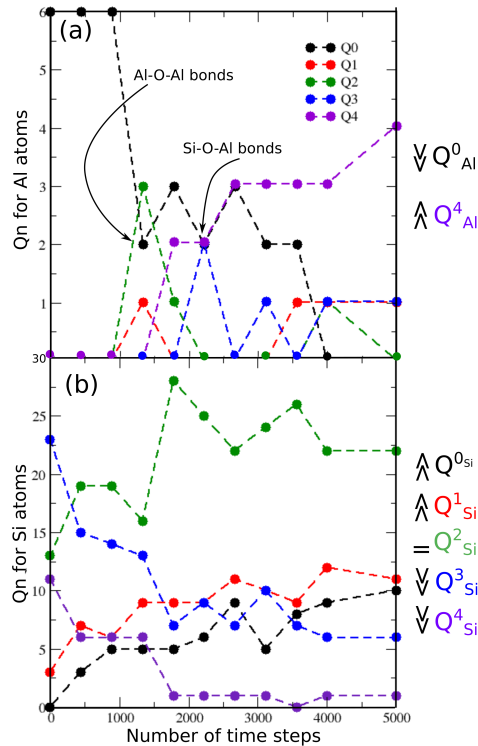
Figure 2. The evolution of (a) Q_{Al}^n and (b) Q_{Si}^n shows that during the first 1000 steps of the simulation, aluminum is only in monomeric form. Note that we consider Al-O-Al, Al-O-Si and Si-O-Si bonds but experimentally by NMR only Si-O-Si and Si-O-Al bonds are measurable. This implies that in figure (a), during the 2000 first steps before the formation of aluminosilicates, Al-O-Al bonds are counted as Q^2 in the aluminate rings. In figure (b), both Al-O-Si and Si-O-Si bonds are counted, the quantity of Al is only 10% of the total number of Si+Al. During this stage, due to the presence of OH groups, silicates start to dissociate, a process that will continue until pure silicates only contains less than 3 members. After 1000 steps, aluminates start to connect to silicate clusters to form aluminosilicates. The quantity of Q_{Al}^4 increases and shows that aluminates are migrating to the center of aluminosilicate clusters and help forming larger clusters than pure silicate ones.

tion process. To recall, the Loweinstein rule states that forming Al-O-Si bonds is always thermodynamically favored over making Al-O-Al bonds for low aluminate concentrations [34], therefore aluminum atoms can not occupy two adjacent tetrahedral sites. As it will be discussed below, the rule is respected due to the reorganization of the aluminosilicate structure after the first Al-O-Si bond is formed. Interestingly, the formation of aluminate

6

structures in solution could explain the appearance of minerals and other structures that breaks the Loweinstein rule in nature[19]. In constrained processes, it is possible that the Al-O-Al bonds that are being formed in the solution cannot be reorganized to form Al-O-Si bonds, which would settle this frustration.

After the connection of the 3-members aluminate cluster with a silicate species, the aluminosilicate will start to reorganize quickly. Aluminate rings are dissociated and the aluminum atoms diffuse in the silicate cluster. This new process for the formation of aluminosilicate entities in solution transforms the cluster in an aluminosilicate in which the network is formed by Si-O-Si and Si-O-Al bridges. This is how the Loweinstein rule is respected in the formation of the aluminosilicates in solution. For this process, the presence of water is necessary as the hydrolysis of the Al-O-Al bonds is the bottleneck to the diffusion of the aluminum atoms into the silicate oligomers to form an aluminosilicate structure.
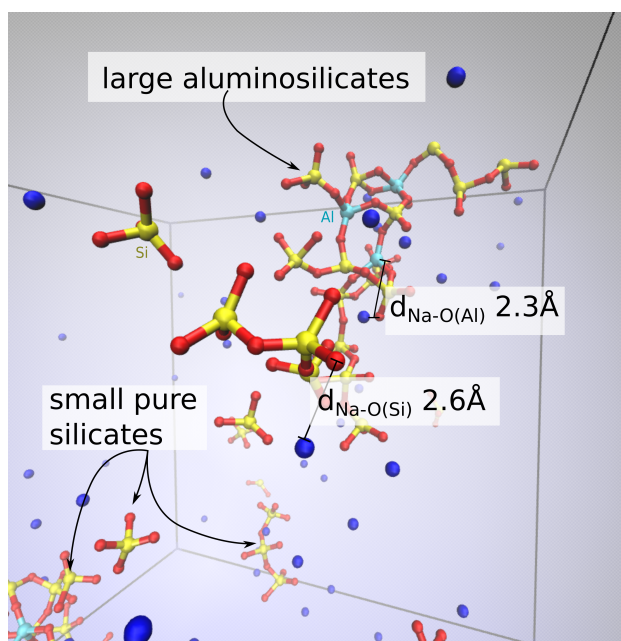
Figure 3. Final structure obtained after 500 ps of simulation time using brief-PT, corresponding to an estimated time of a few seconds, aluminates are connected to 4 Al-O-Si bridges. There is a demarcation between pure silicates that are only in small clusters (monomers, dimers or trimers) and aluminosilicates made of a minimum of 7 Si or Al members. As indicated by the distances written on the figure, the environment in a sphere of 3 $\mathring{A}$ around pure silicates does not contain sodium whereas all aluminosilicates are surrounded by sodium for charge compensation.

In order to follow the evolution of the connectivity, we have computed Q_{Si}^n and Q_{Al}^n, which

corresponds to the number of Si-O-Si (or Al-O-Si) bonds for each Si (or Al) atom. The evolution of Q_{Al}^n, shown in Fig. 2 is characteristic of the process that has been described. In the early stages of the dynamics, the aluminum is in a Q^0 position corresponding to an aluminate monomer. In the simulations, silicon and aluminum atoms always are in a tetrahedral site in agreement with experiments[35]. Part of the aluminum form an aluminate ring cluster that can be seen because of the increase in Q^2 (note that we consider both Si-O-Al and Al-O-Al bonds to calculate Q^2, contrarily to NMR experiments that can only show Si-O-Al connectivity) before 2000 simulation steps. At the end of the trajectory, the majority of the Al is in a Q^4 position and all of them are surrounded by Si only (in agreement with the Lowenstein rule) indicating that they have migrated at the center of the aluminosilicate clusters. Meanwhile, a decomposition of the silicate species is observed (Fig. 2 bottom). In particular, the apparition of Q^0 and Q^1 is explained by the formation of monomers and short silicate chains.

Our results indicate clearly that the aluminate does not serve as the neuralgic center for the growth of aluminosilicate in a nucleation-like process. On the contrary, precursor aluminate and silicate species can be formed prior to the formation of the aluminosilicate clusters and the limiting factor is now the diffusivity of aluminum atoms through the silicate oligomer. Note that only the molecular dynamics enable us to differentiate between a nucleation process or an aggregation process as described herein. Indeed, experimental studies of aluminosilicate tend to show that aluminates are highly connected and are often in a Q^4 position[36, 37], which seemingly indicates that silicates precipitate around an aluminate monomer. In our simulations, the aluminum atom is indeed highly connected after the formation of the aluminosilicate but it is not the result of a nucleation process. Interestingly, we observe that after diffusion of the aluminates into the aluminosilicate structure, the size of the aluminosilicate cluster tends to grow, thus, other silicates species can still connect to the structure.

In Fig. 3, the formation of several entities is observed. Aluminosilicates form large species, which is the result of the polycondensation that is started upon mixing the silicate and aluminate solutions. Meanwhile, pure silicate species that do not contain aluminum, are decondensed by sodium hydroxide[24] and are present only in short chains or single monomers. Therefore, the distribution of silicates and aluminosilicates is polydisperse. As shown on Fig. 3, the sodium remains close to aluminosilicates (at a distance of about 2.3 to

8

2.6Å) and there is no sodium near pure silicates. The two main groups of molecules (small pure silicates and large aluminosilicates) will have distinct superficial charges (that depends on the quantity of aluminum and on the compensation scheme with protonation of oxygen or sodium ions), different masses, and interaction forces. Therefore, the simulations suggest that there should be a phase separation.
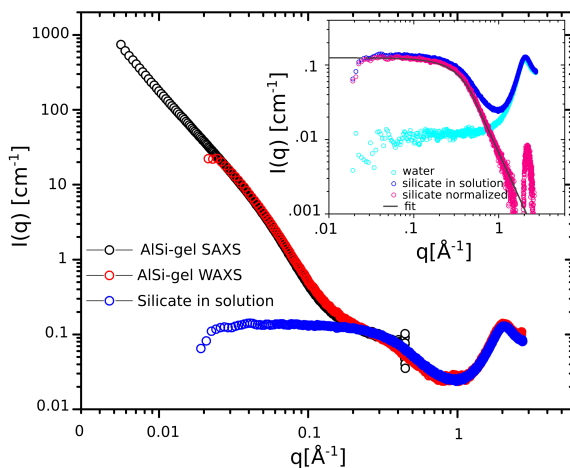
Figure 4. Scattering intensity of an aluminosilicate gel and of the silicate remaining in the solution after the polycondensation reaction measured in Small Angle X-ray Scattering and Wide Angle X-ray Scattering ([21]). The inset focuses on the scattering of the remaining silicate into the solution and the water. The contribution of water was subtracted to isolate the contribution of silicate entities. This latter is fitted by a Guinier-Porod model [38] to compute the radius of gyration R_g=3.8 Å and a Porod exponent = 2.5.

As previously described, our models were built upon the experimental data in terms of chemical composition, the density of the solutions, and NMR measurements, Dupuis et al[21]. In the present experiments, we prepared a gel with a final concentrations of: [Si] = 1.125 mol.L^{-1}, [Na] = 1.31 mol.L^{-1} and [Al] = 0.12 mol.L^{-1} corresponding to Si/Al=9.375 and Na/Al=10.92. The addition of aluminates monomers to the silicate solution initiates the polycondensation reactions to form aluminosilicate entities that grow and interact each other to form a gel[25]. Figure 4 shows the scattering intensity of the gel in SAXS and WAXS configuration. The gel is composed of aluminosilicate building blocks that aggregates with each other to form clusters with a fractal dimension of around 2.1 (for $q \leq 0.1$ Å^{-1}) as described in Keshavarz et al.[25]. In a previous study, we have studied experimentally and

modeled alkali silicate solution having the same proportions Si/Na as our current system but by adding sodium hydroxide instead of aluminates. This sodium hydroxide provokes the decondensation of silicates, [21]. The remaining silicates in solution are observable in Figure 4 where the scattering of silicate overlap perfectly well on the scattering of the gel for $q \geq 0.15$ Å^{-1}. After removing the contribution of the water the scattering of silicates is modeled by a Guinier-Porod model [38], (see the inset in Figure 4). From this model, the radius of gyration R_g=3.8 Å and a Porod exponent $= 2.5$ were obtained. This result is consistent with the size of silicate dimers or cyclic trimers (Si-O distance is about 1.6Å in silicates[39]). The size of the remaining silicate is lower than the aluminosilicate building blocks that are around 15 Å[25]. It confirms here that the two antagonist reactions take place, one that produces the gel due to the polycondensation between silicate and aluminate entities and one that decondensate the silicate that remains suspended in the solution.

With our simulations, we can confirm that aluminum is a strong bond-maker[15] whereas sodium hydroxide is a bond-breaker. We clarify that aluminosilicate chains are being protected by the integration of aluminate. This is due to a more stable Al-O bond compared to Si-O bond, a change in the charge compensation scheme with more sodium in the vicinity of the molecule, and an increase in the connectivity of the molecule that is, therefore, less subject to OH$^-$ attacks. Moreover, the simulation confirms also that the initial concentration of silicates does not react entirely with the aluminates. The presence of aluminates produces some aluminosilicates oligomers of finite size. The final result of the Q_{Al}^n presented in figure 2 is also in agreement with NMR experimental data available in the literature on this kind of gels or on geopolymers. Indeed, it is well known that Al sites are bridged with 4 Al-O-Si as Q_{Al}^4[36, 40]

In the simulations, we observe that the size of the aluminosilicate clusters is dependent on the quantity of Al. As shown in Fig. 5, clusters having no Al have only 1 to 4 members maximum, which indicates that they are primarily targeted by the sodium hydroxide leading to decondensation. On the contrary, the cluster having the maximum number of Al (3 Al and 18 Si) is the largest macromolecule in the system. The increase in size is monotonous and linear with respect to the number of Al. The clusters containing more members also have a larger gyration radius. Unfortunately, it is not possible experimentally to have access to this accurate evolution of sizes since the population of oligomers is averaged by scattering techniques. Only the minimum and maximum mean sizes of polydisperse scatterers are ob-

servable. However, the comparison between simulation and calculated is very good in terms of aluminosilicate and remaining silicates sizes namely around 20 $\mathring{A}$ and 4 $\mathring{A}$ respectively. Due to the effect of the aluminum incorporation in aluminosilicates, the solution contains heavy aluminosilicate aggregates and light short silicate chains. This indicates a phase separation or a demixing due to the different densities of the species and their different affinities. The scattering results suggest this finding (see Figure 4 and Keshavarz et al.[25]) since, after the formation of the gel, we observe an aluminosilicate phase composed of aggregates of the size of about 20 $\mathring{A}$ whereas the floating phase is a pure silicate with only short-range structure. This finding indicates that the complex chemical path that has been described by the simulations is the first step towards the formation of zeolites. However, in the zeolite structure that is formed in the long term with the chemical composition studied here, namely Chabazite, there is a ratio Si/Al = 2, which does not correspond to the initial composition of the solution (Si/Al = 10)[25]. Therefore, demixing is an essential process to reequilibrate the stoichiometry in order to form zeolite compounds with the desired stoichiometry.

To conclude, the decondensation and polymerization, happening simultaneously, of aluminosilicates in an alkali-rich solution has been reproduced for the first time with a fully atomistic calculation concomitantly with experimental synthesis and structural characterization of the hydrogels. Advanced molecular dynamics methods have been used to accelerate the dynamics and classical reactive force fields have been used to take into account the bond-forming and dissociation, essential to study and give some new insights on the polycondensation process from very short timescale to longer times. The process of aluminosilicate formation shows that first aluminates and silicates can be formed independently and are stable in water. Those species start forming clusters when they enter into contact which triggers the diffusion of aluminum atoms into the aluminosilicate species after ring-opening. An aggregation process rather than a nucleation-like one seems then most likely as suggested by the simulation. The Lowenstein rule, which is broken at the moment the macromolecule is formed, is recovered after a few picoseconds. In agreement with experiments and other simulations, this shows that aluminosilicate species are more stable than pure silicates and pure aluminates and are forming larger aggregates in alkali-rich solutions. The size of the cluster is dependent on the number of aluminum atoms that are included in the cluster. Therefore, non-Al containing species will be decondensated due to the presence of sodium hydroxide and form only short polymeric chains or monomers. On the contrary, the species
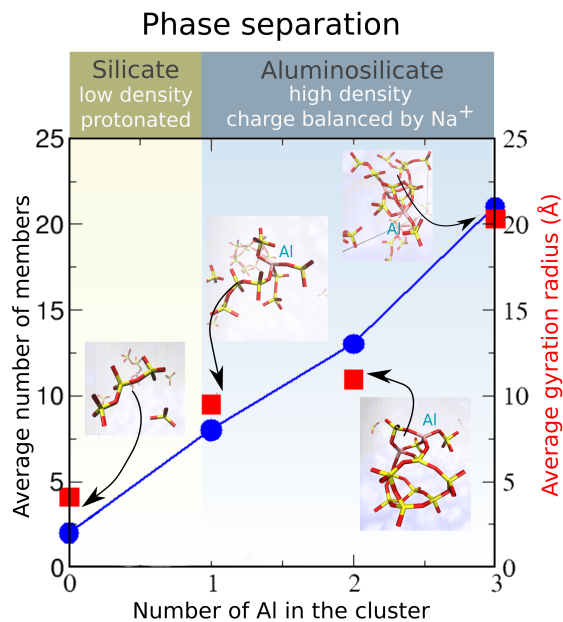
Figure 5. In blue, average cluster size (number of members) versus the number of Al atoms in the cluster in the final configuration. In red, average radius of gyration. The average number of members increases with the number of Al in the aluminosilicate as well as it's gyration radius. The average radius of gyration for pure silicates is 4Å(not considering monomers) which is close to the experimental value of 3.8Å. The difference in environment and size between pure silicates and aluminosilicates indicates that these phases will have significantly different affinity and density, which leads to phase separation. The snapshots are reproduced in larger size in supplemetary materials.

that contains the most Al is composed of more than 20 (Si+Al) atoms indicating the stability of the structure. This result is in extremely good agreement with the experiments showing a phase separation of a heavy aluminosilicate phase and a lighter pure silicate phase containing only short silica chains. This study paves the way to the understanding of the formation of aluminosilicate species in solution that are the precursors of various materials such as zeolites and alkali-activated materials. Further research is needed to confirm the phase separation underlined in this study and the aggregation process between aluminosilicate species forming clusters using fully atomistic large simulations.

---

[1] J. Šefčík and A. V. McCormick, Thermochemistry of aqueous silicate solution precursors to ceramics, AIChE Journal **43**, 2773 (1997).

[2] J. Aupoil, J.-B. Champenois, J.-B. d'Espinose de Lacaillerie, and A. Poulesquen, Interplay between silicate and hydroxide ions during geopolymerization, Cement and Concrete Research **115**, 426 (2019).

[3] S. D. Kinrade and T. W. Swaddle, Silicon-29 nmr studies of aqueous silicate solutions. 1. chemical shifts and equilibria, Inorganic Chemistry **27**, 4253 (1988).

[4] A. V. McCormick, A. T. Bell, and C. J. Radke, Evidence from alkali-metal nmr spectroscopy for ion pairing in alkaline silicate solutions, The Journal of Physical Chemistry **93**, 1733 (1989).

[5] J. W. Phair, J. C. Schulz, L. P. Aldridge, and J. D. Smith, Small-angle neutron scattering and rheological characterization of aluminosilicate hydrogels, Journal of the American Ceramic Society **87**, 129 (2004).

[6] M. Ogura, Y. Kawazu, H. Takahashi, and T. Okubo, Aluminosilicate species in the hydrogel phase formed during the aging process for the crystallization of fau zeolite, Chemistry of Materials **15**, 2661 (2003).

[7] V. Valtchev, G. Majano, S. Mintova, and J. Pérez-Ramírez, Tailored crystalline microporous materials by post-synthesis modification, Chem. Soc. Rev. **42**, 263 (2013).

[8] L. Itani, Y. Liu, W. Zhang, K. N. Bozhilov, L. Delmotte, and V. Valtchev, Investigation of the physicochemical changes preceding zeolite nucleation in a sodium rich aluminosilicate gel,

Journal of the American Chemical Society **131**, 10127 (2009).

[9] P. Steins, A. Poulesquen, O. Diat, and F. Frizon, Structural Evolution during Geopolymerization from an Early Age to Consolidated Material, Langmuir **28**, 8502 (2012).

[10] P. Duxson, A. Fernandez-Jimenez, G. C. Provis, J. L.and Lukey, A. Palomo, and J. S. J. van Deventer, Geopolymer technology: the current state of the art, Journal of Materials Science , 2917 (2007).

[11] J. Rouyer and A. Poulesquen, Evidence of a fractal percolating network during geopolymerization, Journal of the American Ceramic Society **98**, 1580 (2015).

[12] L. N. Assi, K. Carter, E. Deaver, and P. Ziehl, Review of availability of source materials for geopolymer/sustainable concrete, Journal of Cleaner Production **263**, 121477 (2020).

[13] A. Favier, G. Habert, J. d'Espinose de Lacaillerie, and N. Roussel, Mechanical properties and compositional heterogeneities of fresh geopolymer pastes, Cement and Concrete Research **48**, 9 (2013).

[14] C.-S. Yang, J. M. Mora-Fonz, and C. R. A. Catlow, Stability and structures of aluminosilicate clusters, The Journal of Physical Chemistry C **115**, 24102 (2011).

[15] H. Manzano, J. S. Dolado, and A. Ayuela, Aluminum Incorporation to Dreierketten Silicate Chains, The Journal of Physical Chemistry B **113**, 2832 (2009).

[16] C. E. White, J. L. Provis, G. J. Kearley, D. P. Riley, and J. S. J. van Deventer, Density functional modelling of silicate and aluminosilicate dimerisation solution chemistry, Dalton Trans. **40**, 1348 (2011).

[17] C.-S. Yang, J. M. Mora-Fonz, and C. R. A. Catlow, Modeling the polymerization of aluminosilicate clusters, The Journal of Physical Chemistry C **116**, 22121 (2012).

[18] V. O. Özçelik and C. E. White, Nanoscale charge-balancing mechanism in alkali-substituted calcium–silicate–hydrate gels, The Journal of Physical Chemistry Letters **7**, 5266 (2016).

[19] R. Dupuis, J. Moon, Y. Jeong, R. Taylor, S.-H. Kang, H. Manzano, A. Ayuela, P. J. Monteiro, and J. S. Dolado, Normal and anomalous self-healing mechanism of crystalline calcium silicate hydrates, Cement and Concrete Research **142**, 106356 (2021).

[20] T. Du, H. Li, Q. Zhou, Z. Wang, G. Sant, J. V. Ryan, and M. Bauchy, Atomistic origin of the passivation effect in hydrated silicate glasses, npj Materials Degradation **3** (2019).

[21] R. Dupuis, D. G. Rodrigues, J.-B. Champenois, R. Pellenq, and A. Poulesquen, Time resolved alkali silicate decondensation by sodium hydroxide solution, Journal of Physics: Materials **3**

(2019).

[22] R. Dupuis, L. K. Béland, and R. J.-M. Pellenq, Molecular simulation of silica gels: Formation, dilution, and drying, Phys. Rev. Materials **3**, 075603 (2019).

[23] K. Yang, Y. Hu, Z. Li, N. M. A. Krishnan, M. M. Smedskjaer, C. G. Hoover, J. C. Mauro, G. Sant, and M. Bauchy, Analytical model of the network topology and rigidity of calcium aluminosilicate glasses, Journal of the American Ceramic Society **104**, 3947 (2021).

[24] R. Dupuis, R. Pellenq, J.-B. Champenois, and A. Poulesquen, Dissociation mechanisms of dissolved alkali silicates in sodium hydroxide, The Journal of Physical Chemistry C **124**, 8288 (2020).

[25] B. Keshavarz, D. G. Rodrigues, J.-B. Champenois, M. G. Frith, J. Ilavsky, M. Geri, T. Divoux, G. H. McKinley, and A. Poulesquen, Time–connectivity superposition and the gel/glass duality of weak colloidal gels, Proceedings of the National Academy of Sciences **118** (2021).

[26] A. P. Thompson, H. M. Aktulga, R. Berger, D. S. Bolintineanu, W. M. Brown, P. S. Crozier, P. J. in 't Veld, A. Kohlmeyer, S. G. Moore, T. D. Nguyen, R. Shan, M. J. Stevens, J. Tranchida, C. Trott, and S. J. Plimpton, LAMMPS - a flexible simulation tool for particle-based materials modeling at the atomic, meso, and continuum scales, Comp. Phys. Comm. **271**, 108171 (2022).

[27] A. C. T. van Duin, S. Dasgupta, F. Lorant, and W. A. Goddard, Reaxff: A Reactive Force Field for Hydrocarbons, The Journal of Physical Chemistry A **105**, 9396 (2001).

[28] S. H. Hahn, J. Rimsza, L. Criscenti, W. Sun, L. Deng, J. Du, T. Liang, S. B. Sinnott, and A. C. T. van Duin, Development of a reaxff reactive force field for nasiox/water systems and its application to sodium and proton self-diffusion, The Journal of Physical Chemistry C **122**, 19613 (2018).

[29] M. C. Pitman and A. C. T. van Duin, Dynamics of confined reactive water in smectite clay–zeolite composites, Journal of the American Chemical Society **134**, 3042 (2012).

[30] H. Liu, S. H. Hahn, M. Ren, M. Thiruvillamalai, T. M. Gross, J. Du, A. C. T. van Duin, and S. H. Kim, Searching for correlations between vibrational spectral features and structural parameters of silicate glass network, Journal of the American Ceramic Society **103**, 3575 (2020).

[31] M. G. Muraleedharan, H. Asgar, S. H. Hahn, N. Dasgupta, G. Gadikota, and A. C. T. van Duin, Interfacial reactivity and speciation emerging from na-montmorillonite interactions with

water and formic acid at 200 c: Insights from reactive molecular dynamics simulations, infrared spectroscopy, and x-ray scattering measurements, ACS Earth and Space Chemistry **5**, 1006 (2021).

[32] S. Gowtham, K. C. Lau, M. Deshpande, R. Pandey, A. K. Gianotto, and G. S. Groenewold, Structure, energetics, electronic, and hydration properties of neutral and anionic al3o6, al3o7, and al3o8 clusters, The Journal of Physical Chemistry A **108**, 5081 (2004).

[33] R. Dupuis, J. S. Dolado, J. Surga, and A. Ayuela, Doping as a way to protect silicate chains in calcium silicate hydrates, ACS Sustainable Chemistry and Engineering **6**, 15015 (2018).

[34] R. G. Bell, R. A. Jackson, and C. R. A. Catlow, Löwenstein's rule in zeolite A: A computational study, Zeolites **12**, 870 (1992).

[35] C. T. G. Knight, R. J. Balec, and S. D. Kinrade, Aqueous alkali-metal silicate anions containing fully condensed four-coordinate sites, Angewandte Chemie International Edition **51**, 9900 (2012).

[36] J. N. Mills, N. J. Wagner, and P. Mondal, Relating chemical composition, structure, and rheology in alkali-activated aluminosilicate gels, Journal of the American Ceramic Society **104**, 572 (2021).

[37] A. Favier, G. Habert, N. Roussel, and J.-B. d'Espinose de Lacaillerie, A multinuclear static nmr study of geopolymerisation, Cement and Concrete Research **75**, 104 (2015).

[38] B. Hammouda, A new Guinier–Porod model, Journal of Applied Crystallography **43**, 716 (2010).

[39] N. M. Trease, T. M. Clark, P. J. Grandinetti, J. F. Stebbins, and S. Sen, Bond length-bond angle correlation in densified silica—results from 17o nmr spectroscopy, The Journal of Chemical Physics **146**, 184505 (2017).

[40] A. Favier, G. Habert, N. Roussel, and J.-B. d'Espinose de Lacaillerie, A multinuclear static nmr study of geopolymerisation, Cement and Concrete Research **75**, 104 (2015).